

## Observation of Single-Electron Charging Effects in Small Tunnel Junctions

T. A. Fulton and G. J. Dolan

*AT&T Bell Laboratories, Murray Hill, New Jersey 07974*

(Received 6 March 1987)

Unusual structure and large electric-field-induced oscillations have been observed in the current-voltage curves of small-area tunnel junctions arranged in a low-capacitance ( $\lesssim 1$  fF) multiple-junction configuration. This behavior arises from the tunneling of individual electrons charging and discharging the capacitance. The observations are in accord with what would be expected from a simple model of the charging energies and voltage fluctuations of  $e/C$  associated with such effects.

PACS numbers: 73.40.Gk

We have observed prominent structure and striking oscillations in the current-voltage ( $I$ - $V$ ) curves of small-area tunnel junctions arranged in a low-capacitance configuration. This behavior results, we believe, from the tunneling of individual electrons charging and discharging the capacitance, producing discrete voltage jumps of  $e/C$ . A simple model of such charging effects is in accord with the observations. Single-electron charging effects in electron tunneling have long been of interest.<sup>1-10</sup> Previous experiments<sup>1-4</sup> on tunnel junctions containing isolated metal grains within the barrier have observed such effects in an averaged way. Theoretical interest<sup>5-10</sup> has covered single- and multiple-junction configurations with normal and superconducting electrodes.

In the usual picture, an electron passing across the barrier of a tunnel junction gains energy  $eV$ , where  $V$  is the voltage bias and  $e$  is the electronic charge. If the capacitance  $C$  seen by the tunneling electrons is small enough, the charging energy of  $e^2/2C$  also enters in. Considered the circuit model<sup>2,5</sup> on the left of Fig. 1. The tunnel current  $I(V)$  comprises a random flow of discrete charges  $e$  at an average rate  $I(V)/e$ . The current  $I$  is supplied externally to the junction and its inherent parallel capacitance  $C$ . Suppose that initially  $V = V_i > 0$  and an electron tunnels across the barrier. This reduces the charge on  $C$  by  $|e|$  and the voltage to  $V_i - |e|/C$ . The energy gained by the electron,  $|e|V - e^2/2C$ , is given up by the capacitor. This reduction in available energy

from  $|e|V$  impedes the tunneling of electrons having energies below  $e^2/2C$ , producing characteristic structure in the  $I$ - $V$  curve.<sup>1,2,4,5</sup> In particular, for normal electrodes a "Coulomb gap" appears, which comprises an enhanced resistance for  $|V| < |e|/2C$  and a high- $|V|$  offset of  $|e|/2C$ . Subsequently,  $C$  is charged by  $I$  and  $V$  increases until the next electron tunnels, reducing  $V$  by  $|e|/C$ , etc. These fluctuations in  $V$  of  $|e|/C$  tend to broaden structure in the  $I$ - $V$  curves.

To observe charging effects experimentally, we have employed the configuration shown in Fig. 2, in which three junctions of small area, and small overlap capacitance, are formed on a small common electrode. This configuration has low stray capacitance so that the capacitance  $C'$  charged and discharged by the tunneling electrodes is small and well defined, being approximately equal to the sum of the junction capacitances. The behavior in this configuration is similar to that just described although the circuit model, shown on the right of Fig. 1, is more elaborate. The tunneling electrons see an energy cost of  $e^2/2C'$  in tunneling to and from the central electrode, yielding a Coulomb-gap structure in the

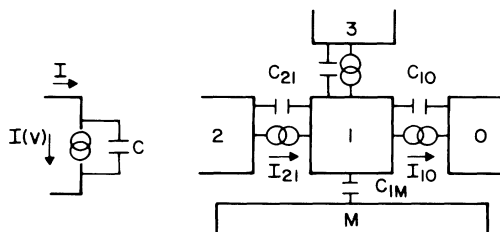


FIG. 1. Left: An equivalent circuit for discussion of charging effects for a single junction. Right: A comparable triple-junction circuit model.

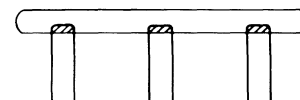
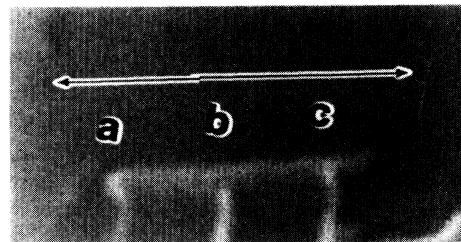


FIG. 2. A scanning-electron micrograph of a typical sample. Junctions labeled a, b, and c are formed where the vertical electrodes overlap and contact the longer horizontal central electrode. The bar is  $1 \mu\text{m}$  long. The configuration is also shown in the accompanying drawing.

$I(V)$  of all the junctions. The voltage of the central electrode,  $V_1$ , jumps back and forth by  $e/C'$  in an erratic telegraphic pattern as the electrons tunnel. A significant additional feature of this configuration is that the charging effects can be modulated periodically by an external electric field, as pointed out by Averin and Likharev.<sup>6</sup>

This classical picture of the behavior becomes inadequate if the average time  $\tau$  that  $V_1$  spends in a state is so short that the lifetime energy broadening,  $\hbar/\tau$ , becomes comparable to the charging energy,  $e^2/2C'$ . Since  $V_1$  changes each time an electron tunnels, the larger currents occurring in lower-resistance junctions give shorter lifetimes. While the value of  $\tau$  depends on the particular state and set of parameters, near the gap region typical junction voltage and current levels are roughly  $e/C'$  and  $e/C'R$  (where  $R$  is the junction resistance), so that  $\tau$  is of order  $RC'$ . Thus to avoid lifetime broadening effects junction resistances should be  $\gtrsim \hbar/e^2$ . For the range of  $C'$  encountered in these experiments this condition also makes the Josephson coupling energy small compared to the charging energy, which suppresses the Josephson effects.

A typical sample is shown in the scanning-electron micrograph and interpretive drawing of Fig. 2. Three adjacent junctions, labeled a, b, and c, share a common central electrode. Measurements are made by the passage of current through, say, junctions a and b and use of c as a probe to monitor the voltage of the central electrode. In this way  $I-V$  curves are obtained for a and b (which contain, however, a voltage contribution from c as mentioned below). The junctions are fabricated by use of a liftoff stencil formed through electron-beam lithography. The Al-Al junctions are formed in a single vacuum cycle using a multiple-angle deposition-oxidation-deposition cycle.<sup>11</sup> Film thicknesses are  $\approx 14$  nm. The junction areas are  $(0.03 \pm 0.01 \mu\text{m})^2$ . The central electrode is  $0.05 \times 0.8 \mu\text{m}^2$ . The substrate is an oxidized silicon wafer with oxide thickness of  $0.44 \mu\text{m}$ . Junction resistances are  $\approx 40$  k $\Omega$ . A Au-Cr film on the back side of the silicon is used to apply an electric field to the central electrode. This sample is one of about twenty fabricated in several different batches. Junction areas ranged from  $0.001$  to  $0.03 \mu\text{m}^2$  and resistances were in the range of  $1$ – $100$  k $\Omega$ , which implies barrier thickness comparable to those commonly encountered in larger junctions. The  $I-V$  curves of these samples were measured in the temperature ( $T$ ) range of  $4.2$ – $1.1$  K.

Three particular phenomena which are expected from the charging effect model are seen in the experimental  $I-V$  curves, becoming especially prominent as the junction areas and hence  $C'$  are reduced. These are the following: (1) A region of increased resistance about  $V=0$  and a high- $V$  offset occur for junctions with normal electrodes, at higher  $T$ . This is the Coulomb-gap structure. (2) As  $T$  is decreased and the electrodes become superconducting, a number of strong, relatively broad bumps

emerge in the  $I-V$  curve in this higher-resistance region. These arise from the superconducting energy-gap structure of the  $I-V$  curves as modified by the charging effects. (3) The shapes of the normal-state  $I-V$  curve in the higher-resistance region and that of the structure in the superconducting state vary periodically with voltage applied to the substrate. This is the oscillatory behavior predicted by Averin and Likharev,<sup>6</sup> for which the period corresponds to the charging of the substrate–central-electrode capacitance  $C_{1M}$  by one electron.

The  $I-V$  curve labeled  $S$  in Fig. 3 shows the characteristic Coulomb-gap structure. This curve is taken at  $1.7$  K for one of the three junctions of a sample of small  $C'$ , closely similar to that of Fig. 2. In contrast, the nearly Ohmic  $I-V$  curve labeled  $L$  is taken at  $1.7$  K for a similar junction cofabricated with  $S$  but having large  $C'$ . The measured  $I-V$  curves involve both the nonlinear junction  $I(V)$  and rectification of the fluctuating voltages by these  $I(V)$ , including that of the probe junction, so that interpretation requires some care. However, from the circuit model one expects (and simulations show) that rectification effects are minor at high biases so that the voltage offset in the Coulomb-gap structure is given by  $e/2C'$ . The offset of  $0.35$ – $0.4$  mV for  $S$  then gives a value of  $C' = 0.20$ – $0.23$  fF. The calculated  $C'$ , based on junction areas of  $(0.03 \pm 0.01 \mu\text{m})^2$  and a thickness-to-dielectric-constant ratio of  $0.15$  nm,<sup>12</sup> is  $0.07$ – $0.28$  fF. The inset of Fig. 3 shows a plot of offset voltage versus total junction areas for this and three other samples. The diagonal line corresponds to a thickness-to-

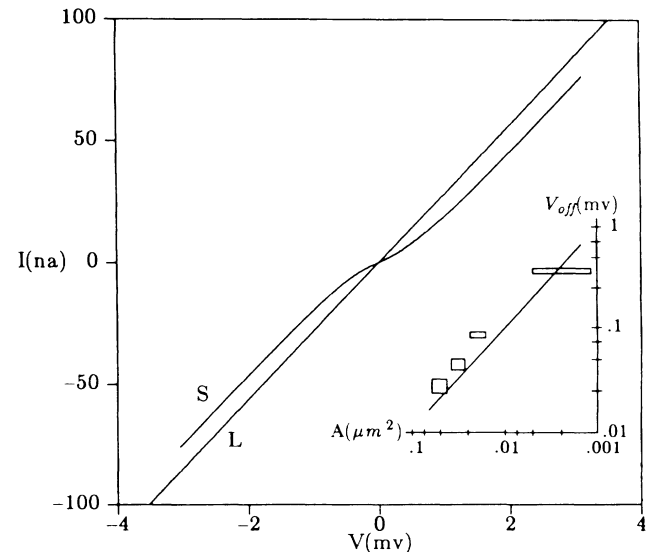


FIG. 3.  $I-V$  curves  $S$  and  $L$  for junctions corresponding to small and large  $C'$  at  $1.7$  K. Inset: Offset voltage vs junction areas (as determined from scanning-electron-microscopy photographs) for four different samples. The boxes represent the estimated uncertainties.

dielectric-constant ratio of 0.15 nm. The agreement is reasonable, but it should be noted that for the smallest junctions the area is not well known while the larger junctions had resistances low enough that lifetime broadening could be a factor.

Figure 4 shows the  $I$ - $V$  curves for junctions  $S$  and  $L$  with superconducting electrodes, at 1.1 K. That for  $L$  resembles those commonly seen for much larger junctions, showing a somewhat broadened current rise at the energy gap of 0.35 mV. For such high-resistance junctions any Josephson supercurrent is suppressed by thermal noise. The  $I$ - $V$  curve for  $S$  shows a less well-defined current rise at a higher voltage, and the shape is asymmetric and contains several broad features. The most striking feature above curve  $S$ , however, is that its detailed shape changes completely upon the application of a voltage to the substrate, in the manner suggested by Averin and Likharev.<sup>6</sup> A manifestation of this is contained in the  $I$ - $V$  curve marked  $SM$  in Fig. 4, taken from junction  $S$ . To produce this curve  $I$  is swept through its range over several minutes while  $V_M$  is varied in a sawtooth manner at  $\sim 0.05$  Hz. The amplitude of  $V_M$  is  $\sim 0.5$  V, over 3 times the voltage (0.14 V) required to produce one complete cycle. Thus the shape of the  $I$ - $V$  curve fluctuates back and forth through six successive cycles fairly rapidly, while  $I$  is swept slowly. This produces the voltage oscillations seen in the curve and shows the degree to which the shape of the curve changes in one cycle. Such oscillations are visible also in the normal state, as shown in the similar curve  $SMN$  taken for this junction at 1.7 K, with use of sweep rates which pro-

duced more closely spaced structure. A portion of the curve at the position of the arrow, expanded by 4 times in both axes, is shown in upper left in Fig. 4. The period of these oscillations did not change between the normal and superconducting states.

A different view of the oscillations is shown for another sample in Fig. 5. The  $I$ - $V$  curve of one junction is shown at five successive values of  $V_M$  increased by increments of  $\approx \frac{1}{6}$  of a cycle. The structure is seen to move along the curve towards positive  $V$ , being relatively sharp at low  $V$  and broadening at higher  $V$ . The inset shows corresponding oscillations in  $V$  vs  $V_M$  for two fixed values of  $I$ .

That the observed period corresponds to  $e/C_{1M}$  was only approximately confirmed. In fact, nominally identical samples had periods in the range 0.03–0.15 V although the period was well defined, constant, and independent of the sample state for a given sample. Our estimate of  $C_{1M}$  for this rather complex geometry is  $7 \times 10^{-18}$  F which may err by factors of 2. This corresponds to  $e/C_{1M} = 0.020$  V which is in fair agreement only with the lowest observed period. We believe that the variations in nominally identical samples and the tendency toward effective capacitances lower than the estimated value are associated with the low-temperature behavior of the lightly doped silicon-silicon-dioxide substrate but further experiments are necessary to clarify this.

Simulations using the model of Fig. 1 give behavior which qualitatively is much like that in Figs. 3–5. Space precludes full discussion, but we sketch briefly how the

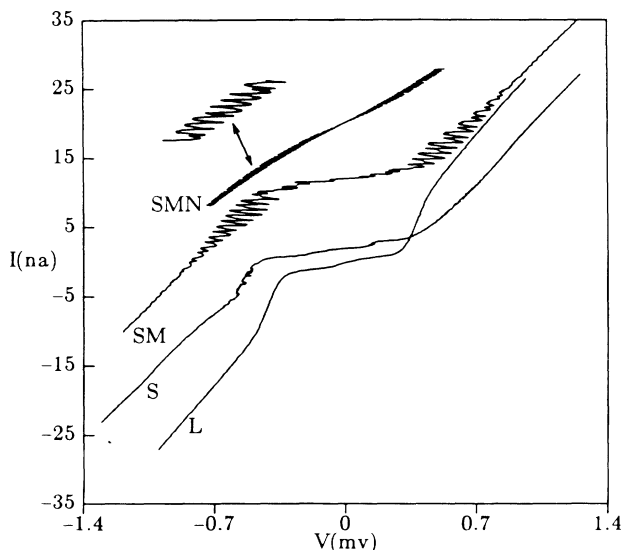


FIG. 4.  $I$ - $V$  curves  $S$  and  $L$  are for the same samples as Fig. 3 but at  $T=1.1$  K.  $I$ - $V$  curves  $SM$  and  $SMN$  show the oscillatory behavior at  $T=1.1$  K and  $T=1.7$  K, as described in the text. Curve  $S$  is offset by 2 nA,  $SM$  by 12 nA, and  $SMN$  by 20 nA.

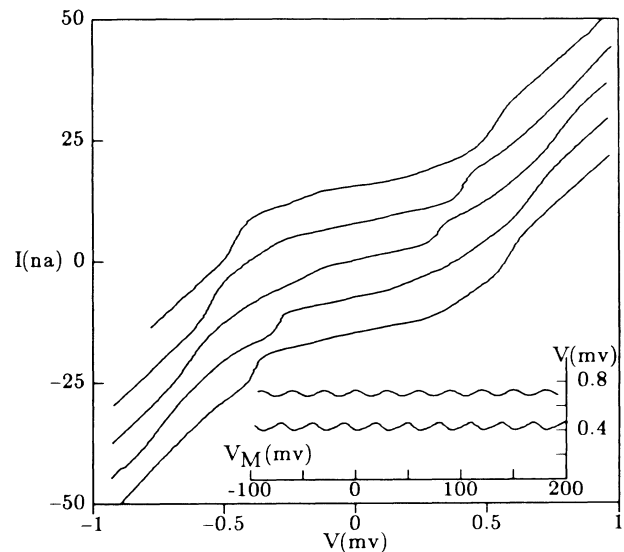


FIG. 5.  $I$ - $V$  curves for a sample at  $T=1.1$  K for a set of equally spaced substrate biases covering  $\frac{1}{6}$  of a cycle. Curves are offset by increments of 7.5 nA. Inset:  $V$  vs  $V_M$  for two fixed currents  $I=10.5$  and 26 nA.

oscillations and bumps come about. We neglect the third junction for simplicity, as the behavior is similar. The central electrode voltage  $V_1$  can take only the discrete values  $V_1 = Ne/C' + \alpha V_M + \beta V_2$ , where  $N$  is the number of electrons on the central electrode,  $V_2$  is the voltage of the leftmost electrode,  $V_M$  is the substrate voltage, and  $\alpha$  and  $\beta$  are ratios of capacitances. (Voltages are referenced to the right-most electrode.) Suppose  $V_2$  and  $V_M$  are fixed. Each junction randomly passes electrons at a rate given by its  $I(V)$  (which includes a Coulomb gap) and bias. This causes  $N$ , and  $V_1$  and the junction biases, to jump randomly between a few adjacent allowed values. The average junction current  $I$  is the sum of the current in these states weighted by their occupation. Varying  $V_M$  shifts the allowed  $V_1$  and biases, changing  $I$ . The variation is periodic because the allowed values repeat when  $V_M$  changes by  $e/C_{1M}$ . The current step in  $I(V)$  at the superconducting energy gap produces corresponding bumps in  $V_2$  vs  $I$  at those  $V_2$  for which one of the several levels visited by a junction bias in its random variation falls at the gap. Again, such features shift with changes in  $V_M$ , as in Fig. 5.

In general, then, the behavior shown in Figs. 3–5 agrees qualitatively and semiquantitatively with the charging interpretation. A more detailed comparison should ultimately be made through simulations of the time-dependent behavior with use of the three-junction circuit models. Generally, however, we would conclude that we have clearly seen the Coulomb-gap structure and the electronic-field-induced oscillations as well as the associated ladder structure of allowed voltages. Attempts to see directly the rather rapid voltage jumps which must be occurring among these levels (8 nA corresponds to 100 GHz) by synchronizing them with applied microwaves have not succeeded so far.

To sum up, the low-capacitance multiple junctions de-

scribed here show striking behavior in the  $I$ - $V$  curve in both the normal and superconducting states. The behavior corresponds closely to predictions of a simple model of single-electron charging effects. Some applications in metrology, instrumentation, and computational circuitry are conceivable. Interesting directions to extend this work are the study of competition with Josephson effects and of the role of lifetime broadening

We gratefully acknowledge technical assistance from J. H. Dunsmuir and L. N. Dunkleberger, computational assistance from R. C. Fulton, and helpful conversations and loan of equipment from M. Gurvitch, G. E. Blonder, C. C. Grimes, and A. F. Hebard.

<sup>1</sup>I. Giaever and H. R. Zeller, Phys. Rev. Lett. **20**, 1504 (1968).

<sup>2</sup>H. R. Zeller and I. Giaever, Phys. Rev. **181**, 789 (1969).

<sup>3</sup>J. Lambe and R. C. Jaklevic, Phys. Rev. Lett. **22**, 1371 (1969).

<sup>4</sup>R. E. Cavicchi and R. H. Silsbee, Phys. Rev. Lett. **52**, 1453 (1984).

<sup>5</sup>D. V. Averin and K. K. Likharev, J. Low Temp. Phys. **62**, 345 (1986).

<sup>6</sup>D. V. Averin and K. K. Likharev, in *SQUID '85: Superconducting Quantum Interference Devices and Their Applications* edited by H.-D. Hahlbohm and H. Lubbig (de Gruyter, Berlin, 1986).

<sup>7</sup>E. Ben-Jacob and Y. Gefen, Phys. Lett. **108A**, 298 (1985).

<sup>8</sup>T. L. Ho, Phys. Rev. Lett. **51**, 2060 (1983).

<sup>9</sup>E. Ben-Jacob, E. Motolla, and G. Schon, Phys. Rev. Lett. **51**, 2064 (1983).

<sup>10</sup>M. Buttiker, Phys. Scri. **T14**, 82 (1986).

<sup>11</sup>G. J. Dolan, Appl. Phys. Lett. **31**, 337 (1977); G. J. Dolan, R. E. Miller, R. A. Linke, T. G. Phillips, and D. P. Woody, IEEE Trans. Mag. **17**, 684 (1981); D. J. Bishop, J. C. Licini, and G. J. Dolan, Appl. Phys. Lett. **46**, 1000 (1985).

<sup>12</sup>M. Gurvitch, M. A. Washington, and H. Huggins, Appl. Phys. Lett. **42**, 472 (1983).

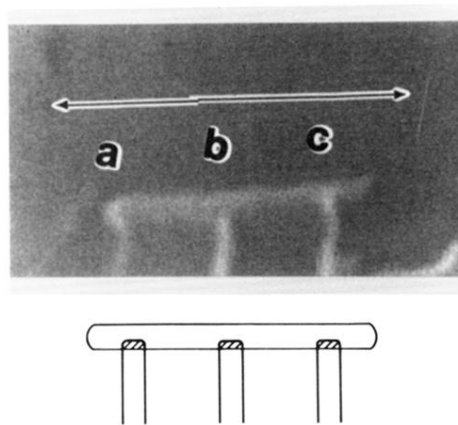


FIG. 2. A scanning-electron micrograph of a typical sample. Junctions labeled a, b, and c are formed where the vertical electrodes overlap and contact the longer horizontal central electrode. The bar is  $1\ \mu\text{m}$  long. The configuration is also shown in the accompanying drawing.